High Resolution Raman and Neutron Investigation of Mg(BH4)(2) in an Extensive Temperature Range

ARTICLE *in* THE JOURNAL OF PHYSICAL CHEMISTRY A · FEBRUARY 2010

Impact Factor: 2.69 · DOI: 10.1021/jp911175n · Source: PubMed

High Resolution Raman and Neutron Investigation of $Mg(BH_4)_2$ in an Extensive Temperature Range

A. Giannasi,* D. Colognesi, L. Ulivi, and M. Zoppi

Consiglio Nazionale delle Ricerche, Istituto dei Sistemi Complessi, Via Madonna del Piano 10, I-50019, Sesto Fiorentino, Italy

A. J. Ramirez-Cuesta

Rutherford Appleton Laboratory, ISIS Facility, Chilton, Didcot, Oxon, OX11 0QX, United Kingdom

E. G. Bardají, E. Roehm, and M. Fichtner

Karlsruhe Institute of Technology, Institute of Nanotechnology, Hermann-von-Helmholtz-Platz 1, 76347 Eggenstein-Leopoldshafen, Germany

Received: December 1, 2009; Revised Manuscript Received: January 13, 2010

Raman spectra of $Mg(BH_4)_2$ have been measured in an extensive temperature range, from 15 to 473 K. Taking into account the high temperature conversion from the α to the β phase, we have observed evident signatures of this phase transition and determined the Raman vibrational spectrum of each phase. The neutron scattering spectra of the β phase sample were also recorded. The present experimental results have been compared to the density functional theory calculations available in the literature, and a substantial agreement has been found.

I. Introduction

Given its high gravimetric hydrogen content (14.9 mass %), magnesium borohydride is considered a promising material for mobile hydrogen storage applications. According to recent investigations performed by Chlopek et al.[1] and Soloveichik et al.,[2] magnesium borohydride releases up to 14.4 mass % of hydrogen upon heating to 800 K, i.e., near the theoretical value. Moreover, its decomposition pathway resulted to be more complex than the simple one originally supposed by Konoplev et al.,[3] passing through four different decomposition steps and forming several polyborane intermediate species. The rehydration process has been recently investigated by Li et al.:[4] it has been demonstrated that the rehydrided sample could reload up to 6.1 mass % through the formation of the $Mg(B_{12}H_{12})$ polyborane.

Depending on the synthesis condition, $Mg(BH_4)_2$ crystallizes in two different phases that have been recently determined by X-ray diffraction (XRD) and neutron diffraction (ND) by Her et al.[5] and Filinchuk et al.[6] The α phase turns out to be characterized by a very complex hexagonal lattice belonging to the $P6_122$ space group, while the β phase shows an orthorhombic primitive cell with a *Fddd* symmetry. The α phase is formed by MgH_8 polyhedra almost linearly coordinated by H_2BH_2 units and organized into a three-dimensional network by five-membered $(-Mg\text{-}BH_4-)_n$ rings. The β phase results to be built up by two different MgH_8 polyhedra coordinated by $(-Mg-BH_4-)_n$ rings, where the *n* indices cannot assume odd values.[6]

At ambient pressure the α phase transforms into the β phase at $T = 470$ K. Upon lowering the temperature, the β phase does not transform back into the α phase, due to an extremely slow kinetics, and the system remains in a β phase metastable state.[6]

Room temperature Raman spectra of $Mg(BH_4)_2$ have been reported in the literature at ambient pressure[6,7] or as a function of pressure.[8] To our knowledge, no low temperature Raman spectra have been reported so far. Here we present the low temperature spectra of $Mg(BH_4)_2$ (α and β phases) in the spectral region between 150 and 2500 cm^{-1}. As we will show in the following, the lattice modes of $Mg(BH_4)_2$ in both crystalline phases are well resolved and distinguishable. The same applies to the bending and stretching modes of the B−H vibrations.

The present Raman measurements have been complemented by an incoherent inelastic neutron scattering (IINS) experiment. In this case the measured spectrum is representative of the proton dynamics in the sample, and its interpretation turns out to be more direct. However, due to the presence of a non-negligible momentum transfer, inherent to this class of experiments, the comparison of the spectra belonging to the two different techniques can effectively be carried out in a limited energy range.

II. Experimental Section

A sample of $Mg(BH_4)_2$ was produced at the Karlsruhe Institute of Technology starting from magnesium hydride and triethylamine borane complex as described in ref 1. Structural characterization, using X-ray powder diffraction, was performed in a Philips X'PERT diffractometer (Cu, Kα radiation). The sample powder was spread on a silicon single crystal and sealed in the glovebox with an airtight hood of kapton foil. The analysis of the XRD pattern showed a mixture of α and β phases with a dominating contribution from the α phase (see Figure 1). Elemental analysis gave a hydrogen content of 14.5 mass % (to be compared to the theoretical value of 14.9 mass %). The sample was also analyzed by Fourier transform infrared spec-

* To whom correspondence should be addressed. E-mail: alessandra.giannasi@fi.isc.cnr.it.

10.1021/jp911175n
Published on Web 02/08/2010

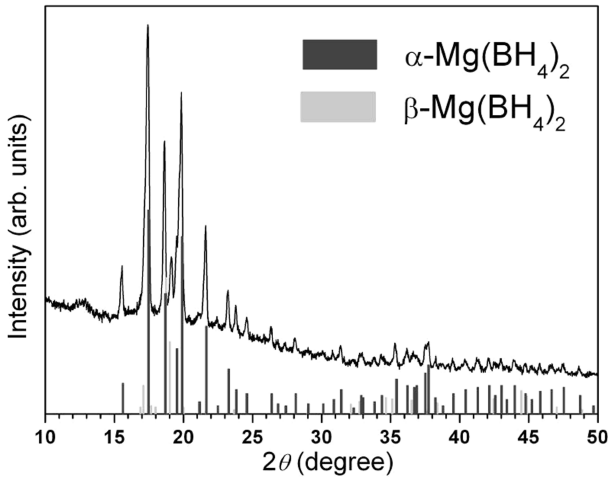

Figure 1. X-ray diffraction pattern of the magnesium borohydride sample showing the presence of both α and β phases, with a dominant contribution from the α phase.

troscopy (FTIR) showing the typical features of a borohydride compound, together with some trace of residual hydrocarbon (C−H stretching vibration in the region around 3000 cm^{-1}; see Figure A in the Supporting Information).

A small amount (namely, 20 mg) of this specimen was carefully transferred into an optical scattering cell using a controlled atmosphere environment (a glovebox filled with pure nitrogen) with a measured content of water and oxygen lower than 0.1 ppm. The sealed scattering cell was then moved to the light scattering apparatus[9] for further conditioning and in situ spectroscopic analysis. The sample cell was first evacuated, using a turbo-molecular pump connected to a clean baking pump, and then filled with helium gas at 4 bar pressure. The presence of helium increases the thermal exchange of the sample with the environment, thus avoiding, or at least greatly reducing, the local heating possibly induced by the laser beam. The spectroscopic Raman measurements were carried out using either the green line ($\lambda = 514.5$ nm) or the blue line ($\lambda = 488.0$ nm) of an argon ion laser. For the reasons mentioned above, the laser power on the sample was kept rather low, close to 1 mW. Spectra were obtained using a Spex Triplemate spectrometer, equipped with high resolution holographic gratings, and recorded using a liquid nitrogen cooled charge coupled device (CCD) camera (Symphony Horiba Jobin Yvon). The overall spectra resolution was about 1.3 cm^{-1}.

a. Room Temperature and Cold ($T = 15$ K) Sample Raman Spectra. Initially, we have carried out a series of Raman measurements on the $Mg(BH_4)_2$ sample as received. In Figure 2 we report the average of several spectra taken at room temperature in the interval 150−2500 cm^{-1}. At low frequency we clearly distinguish three intense lines: a single mode at 170 cm^{-1}, a doublet composed of two distinct peaks at 200 and 207 cm^{-1}, and another single mode at 256 cm^{-1}. A much weaker lattice mode at 344 cm^{-1} is also visible, while some broader structures can be observed in the region between 430 and 700 cm^{-1}. At higher frequencies, we can observe the internal modes of the $[BH_4]^-$ anion. These are the bending modes of the B−H bonds and are composed of a line, located at about 1120 cm^{-1}, a band (including at least two lines) at about 1200 cm^{-1}, and a broad line at about 1400 cm^{-1}. Finally, at even higher frequencies, we see the broad band, extending from 2100 to 2500 cm^{-1}, representing the manifold of the stretching vibrations, together with some combination and overtone bands. The present results are in good quantitative agreement with the previous measurements reported in the literature.[6−8]

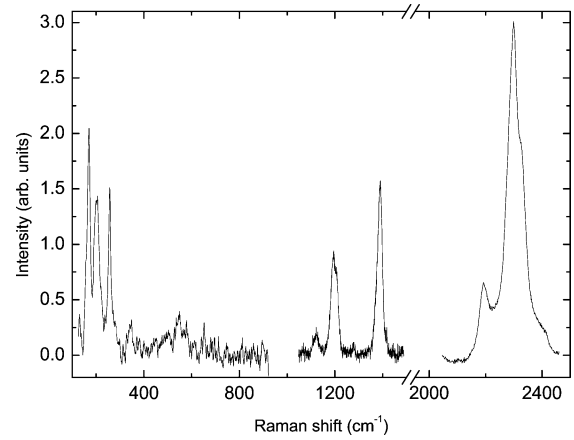

Figure 2. Raman spectrum of magnesium borohydride at room temperature ($T = 295$ K) in the spectral range 150−2450 cm^{-1}. The intensities of the different portions of the spectrum have been scaled differently for graphic reasons.

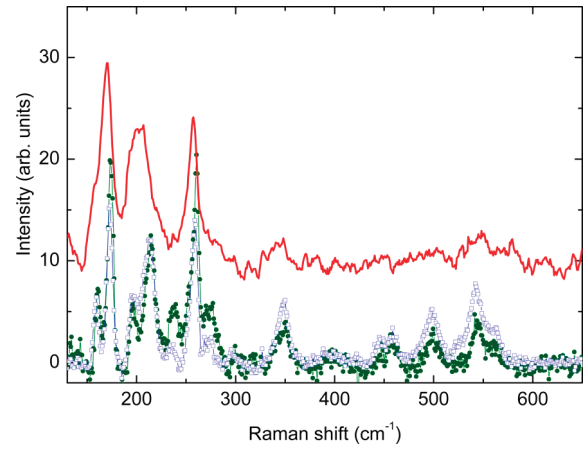

Figure 3. Raman spectrum of magnesium borohydride at $T = 15$ K in the spectral range 150−650 cm^{-1}. The two lowest spectra (line plus symbols) were acquired using two different laser wavelengths, namely, 514.5 nm (green full dots) and 488.0 nm (blue open squares). The uppermost line (red) represents the room temperature spectrum.

Lowering the temperature of the sample allows a significant reduction of the width of the spectral components. Thus, we cooled the sample down to $T = 15$ K, looking for a more detailed peak discrimination and, possibly, a more precise assignment accounting for the different phases. In Figure 3 we show the low temperature spectrum of the lattice modes between 150 and 650 cm^{-1}. We observe that the spectral features appear much more resolved, as expected, while the broad bands in the room temperature spectrum evolve into sharp Raman peaks. We point out that, in order to check the reliability of our results, the two low temperature spectra were collected using two different laser wavelengths, namely, $\lambda = 488.0$ and 514.5 nm. The positive comparison between the two independent spectra unequivocally confirms the reliability of the measured intensity and frequency for each spectral component.

Significant differences are also observed in the spectral region of the bending modes (see Figure 4) where the low temperature spectrum reveals much more resolved peaks than the corresponding room temperature one. In particular, the broad line at 1200 cm^{-1}, observed at room temperature, clearly shows the presence of two separated peaks while the line at about 1400 cm^{-1} appears more asymmetric, suggesting the presence of a doublet. Finally, the low temperature B−H stretching band reveals a much more complex structure with respect to the simpler four-peak structure observed at room temperature.

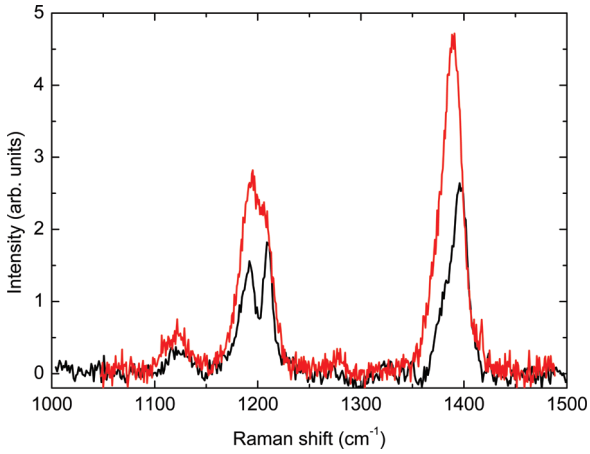

Figure 4. BH bending spectral region at $T = 15$ K (black line) and at room temperature (red line).

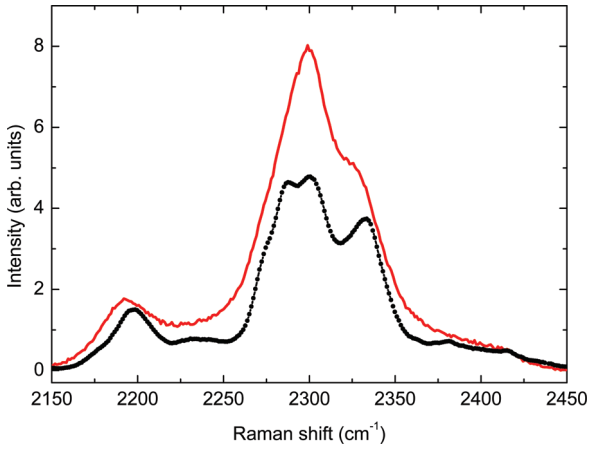

Figure 5. BH stretching spectral region at $T = 15$ K (black dots) and at room temperature (red full line).

This is shown in Figure 5, where we compare the spectrum measured at $T = 15$ K to the room temperature one.

b. Monitoring the α to *β* Phase Transition through Raman Scattering. As reported by Filinchuk and co-workers,[6] the α phase of $Mg(BH_4)_2$ transforms into the more stable β phase in the temperature interval between 490 and 500 K. This phase transformation is not reversible by cooling the sample back to room temperature. Thus, in order to convert our mixed-phase sample into a single phase one, we heated it in helium atmosphere up to the transition temperature, keeping it at $T =$ 500 K for 30 min. The Raman spectra were acquired in situ at different temperatures during this thermal cycle. Then, the cell was cooled again down to $T = 15$ K in order to obtain the expected line narrowing. We found that the final low temperature spectrum appears rather different from that of the mixed phase.

The B−H stretching spectral region is plotted in Figure 6. Here we show the evolution of the Raman spectrum consequent to the temperature changes of the sample. The sequence starts from the bottom, where we report the vibrational spectrum of the pristine material taken at 15 K (the same spectrum as that shown in Figure 5), then the one at room temperature ($T = 298$ K), and then various spectra taken at 423, 453, and 473 K. Subsequently, the sample was cooled down to room temperature (the sixth spectrum) and finally to $T = 15$ K. Thus, the three uppermost spectra in the figure represent the B−H stretching modes relative to the β phase only.

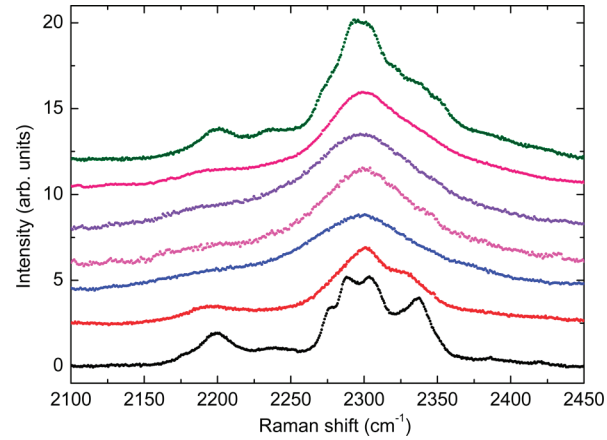

Figure 6. BH stretching spectral region from $T = 15$ K up to the phase transition temperature ($T = 473$ K) and back to 15 K. The recorded spectra correspond (from bottom to top) to 15, 298, 423, 453, 473, 298, and 15 K (see main text for details).

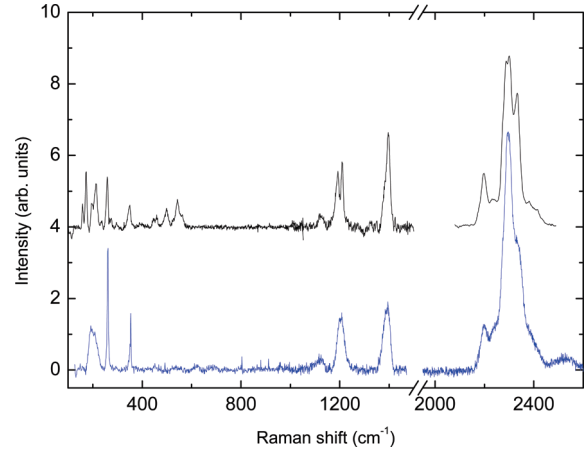

Figure 7. Full Raman spectra at $T = 15$ K of the magnesium borohydride β phase (blue line) and the mixed (α plus β) phase (black line).

The low temperature ($T = 15$ K) full Raman spectrum of the β phase, ranging between 150 and 2500 cm^{-1}, is shown in Figure 7 and compared with the corresponding mixed-phase spectrum (shifted in the figure). The differences are clearly evident. In particular, we observe a drastic change in the region of the lattice modes (150−900 cm^{-1}) and a large modification in the region of the B−H stretching.

c. Neutron Scattering Experiment. Neutron scattering measurements were carried out using the TOSCA-II inelastic spectrometer of the ISIS pulsed neutron source at Rutherford Appleton Laboratory (Chilton, Didcot, U.K.). TOSCA-II is a crystal-analyzer inverse-geometry spectrometer,[15] where the final neutron energy is selected by two sets of pyrolytic graphite crystals placed in forward-scattering (at about 42.6° with respect to the incident beam) and in backscattering (at about 137.7° with respect to the incident beam). This arrangement sets the nominal scattered neutron energy to $E_1 = 3.35$ meV (forward-scattering) and to $E_1 = 3.32$ meV (backscattering). Higher order Bragg reflections are filtered out by 120 mm thick beryllium rods wrapped in cadmium foil and cooled down to a temperature lower than 30 K. The incident neutron beam spans a broad energy range allowing coverage of an extended energy transfer ($E = E_0 - E_1$) region: 3 meV < E < 500 meV. Because of the fixed geometry of this spectrometer, the wave-vector transfer, Q, is related to the energy transfer through a monotonic function, roughly proportional to the square root of the incoming neutron

TABLE 1: Vibrational Frequency Shifts (in cm^{-1}) of $Mg(BH_4)_2$ [a]

assigned mode	present exp.	exp.[7]	exp.[8]	exp.[6]
lattice	170	172	170	−
lattice	200	195	200	−
lattice	207	204	210	−
lattice	256	248	−	−
lattice	344	−	350	−
lattice	430−600 bands	670	−	−
ν_4	1122	1126	1120	−
ν_4	1191	1190	−	1199
ν_4	1208	1205	1210	−
ν_2	1390	1388	1400	1395
$2\nu_4$	2194	−	−	2199
ν_3	2297	2283	2300	2305
ν_1	2332	2334	2340	2330
$\nu_2 + \nu_4$	2400	2383	2360	2400

[a] All the reported Raman frequencies are recorded at room temperature.

TABLE 2: Vibrational Frequency Shifts in $Mg(BH_4)_2$ [a]

modes ($\alpha + \beta$ phase)	fitted frequencies (cm^{-1})	calculated frequencies (cm^{-1})[21,22]
lattice	159, 173, 197, 212, 235, 258, 274, 297, 347, 394, 445, 459, 498, 524, 543, 563	40 modes between 227 and 986
bending		
ν_4	1122, 1190, 1211,	20 modes between
ν_2	1382, 1397	1057 and 1384
stretching		
ν_3	2275, 2288, 2304,	20 modes between
ν_1	2327, 2338	2327 and 2433
combinations and overtones		
$2\nu_4$	2199, 2239, 2390,	
$\nu_2 + \nu_4$	2420	−

[a] The Raman spectrum ($\alpha + \beta$ phase) is recorded at $T = 15$ K. The fitted peak positions are independent of the exciting wavelength (see main text).

energy: $Q = Q_{F,B}(E_0) \propto E_0^{1/2}$ (where suffixes F or B stand for forward-scattering or backscattering, respectively). TOSCA-II has an excellent energy resolution in the accessible energy transfer range ($\Delta E/E_0 \simeq 1.5-3\%$). The scattering cell used for the β-Mg $(BH_4)_2$ sample was made of aluminum with a slab geometry (41 × 43 mm^2, 0.5 mm thick, 1.0 mm of internal gap). Before the actual magnesium borohydride measurement, the empty cell was cooled down to the low temperature value of the experiment, and its time-of-flight spectrum was recorded for a time corresponding to an *integrated proton current* (IPC) of 1623.70 μA h. Special care was taken to prevent possible borohydride wetting and oxidation during the sample loading procedure, performed in an inert-gas glovebox. The sample consisted of 250 mg of $Mg(BH_4)_2$, in the form of a fine polycrystalline powder, that had been previously thermally treated under vacuum up to 573 K, at a heating rate of 2.5 K/min, and then cooled down to room temperature in order to convert it completely into the beta phase. According to XRD and FTIR measurements, performed after the thermal treatment but before the neutron experiment, the sample was not decomposed. The scattering cell, filled with the $Mg(BH_4)_2$ powder, was placed into the cryostat, and the sample measurement was started when the temperature reached 20 K. The stability of the temperature conditions during the whole experiment was not regarded as particularly important, and the cryostat was left slowly reaching its base temperature $T \simeq 12$ K. In this way the average temperature of each individual run is estimated to be $T = (16 \pm 2)$ K. The magnesium borohydride time-of-flight spectrum was recorded for a time corresponding to an IPC of 2000.14 μA h.

III. Data Analysis

a. Raman Data Analysis. The spectra of the $Mg(BH_4)_2$, of both the mixed and the β phases, have been fitted by Lorentzian line shapes. The low frequency region is characterized by the optical modes of the Mg^+ and $[BH_4]^-$ ions (200−300 cm^{-1}) and by the librational modes of the $[BH_4]^-$ anion (∼350 cm^{-1}).[10] The internal modes of the $[BH_4]^-$ anion, namely, the B−H bending (ν_2 and ν_4) and stretching (ν_1 and ν_3), are located at about 1200−1400 cm^{-1} and 2300 cm^{-1}, respectively. First we have analyzed the mixed-phase sample, mainly composed of the α phase. In the region of the lattice modes (150−400 cm^{-1}), we determine the presence of five Raman lines, in quantitative agreement with the published data (see Table 1). As previously stated, the low temperature spectrum evidences some features that could not be revealed at room temperature. For example, the room temperature peak at 170 cm^{-1} splits into two components at 159 and 173 cm^{-1}. The peak at 200 cm^{-1} shifts to 197 cm^{-1}, while the one at 207 cm^{-1} translates to 212 cm^{-1}. The 256 cm^{-1} room temperature peak shifts to 258 cm^{-1}, and three extra peaks at 235, 274, and 297 cm^{-1} appear in the low temperature spectrum. The broad band at about 344 cm^{-1} becomes a distinct line at 347 cm^{-1}. Moreover, the broad structure observed between 430 and 600 cm^{-1} in the room temperature spectrum gives rise to six distinct peaks that could be related to overtones and combination bands of the external vibrations (see Table 2 for details). We point out that, while decreasing temperature, we have not observed in the measured spectra any sudden change suggestive of a possible phase transition. Thus, we ascribe the bands, observed at the various temperatures, to the same vibrational modes. Obviously, due to low temperature hindering of several relaxation mechanisms, the resulting spectral bands appear much narrower.

As for the bending region, the low temperature spectrum fit evidences three peaks (namely at 1122, 1190, and 1211 cm^{-1}), which are attributed to the ν_4 vibrational mode, while the two former lines appeared much less distinguishable in the room temperature spectrum. The fitted modes at 1382 and 1397 cm^{-1} are attributed to the ν_2 vibration, which was fitted by a single line (at 1390 cm^{-1}) in the room temperature spectrum. A similar large splitting of the ν_4 mode has been observed in $LiBH_4$ by Racu et al.[11]

For the B−H stretching of the mixed phase, we have decided, consistently with the spectral detail and the noise level of the experimental data, to use nine components for the fit. We observe that the ν_3 antisymmetric stretching mode, located at about 2297 cm^{-1} in the room temperature spectrum, turns out to be composed of at least three different features (see Figure 5). Moreover, the ν_1 symmetric stretching mode, which appears as a shoulder on the high frequency side of the main room temperature peak, is made of two components (cf. Table 2). The manifold of the symmetric and antisymmetric modes can be attributed to the degeneracy lifting due to site group splittings, while, as mentioned in the literature,[12] the correlation field effect (related to the presence of more than one anion in the unit cell) does not appear to give measurable shifts in simpler borohydride systems.

As in similar borohydride-based solids,[13] the frequency of the bending mode first overtones is found rather close to the

TABLE 3: Vibrational Frequency Shifts of the $Mg(BH_4)_2$ Metastable β Phase[a]

modes β	fitted frequencies (cm^{-1})
lattice	192, 208, 222, 261, 295, 353 450, 491, 527 620, 685
bending	
ν_4	1117, 1204
ν_2	1390
stretching	
ν_3	2296
ν_1	2346
combinations and overtones	
$2\nu_4$	2198, 2232
$\nu_2 + \nu_4$	2395, 2534

[a] Raman spectra have been recorded at $T = 15$ K after the thermal treatment to induce the transition to the β phase. We note that the number of the observed lattice modes is drastically reduced with respect to the mixed phase (cf. Table 2).

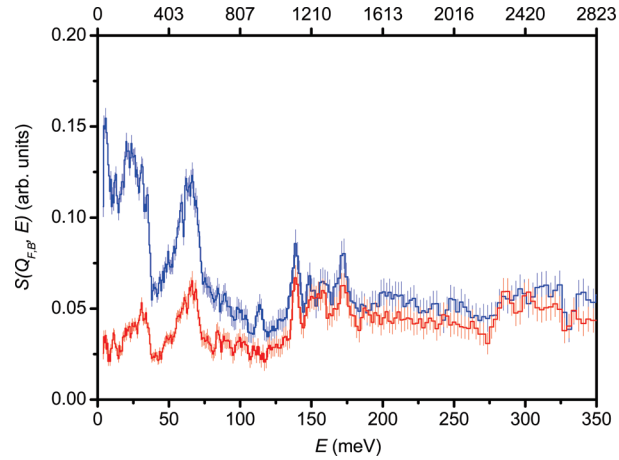

Figure 8. Generalized self-inelastic structure factor from thermally treated $Mg(BH_4)_2$ (β phase) recorded on TOSCA at $T = 16 \pm 2$ K in backscattering (blue histogram and error bars) and in forward-scattering (red histogram and error bars). On top of the figure, the energy shift scale has been converted to cm^{-1}.

fundamental B−H stretching vibration, giving rise to a Fermi resonance. Carbonniere et al.[13] have demonstrated that for metal borohydrides such an effect is not negligible. Thus, referring to the main component of the mode, we assign the structures at 2199 and 2239 cm^{-1} in the low temperature spectrum to the $2\nu_4$ overtone. The two peaks at 2390 and 2420 are attributed to the $\nu_2 + \nu_4$ combination bands.[13,14] Results are summarized in Table 2.

In the pure β phase, the spectrum exhibits the main differences, with respect to the mixed phase, in the low frequency region. Sixteen modes were detected in the mixed-phase sample, while only two well-defined peaks and one broader band appear in the spectrum of the β phase. The supposed combination and overtone bands turn out to be very weak and the related spectrum very noisy. Nevertheless at least five peaks have been fitted. Results are reported in Table 3. As for the bending modes, we have used five components for the mixed phase, while only three were employed for the β phase spectrum. The stretching region has been fitted using six Lorentzian components. Two were attributed to the B−H vibrations and the other four to the combination and overtones bands. It is interesting to observe that, while the average B−H stretching frequency does not change significantly going from the mixed to the β phase, the intensity distribution does, suggesting a different spatial distribution of the $[BH_4]^-$ tetrahedra in the two crystalline structures. The comparison between the Raman spectra of the pristine material and the pure β phase substantially confirmed the XRD investigation results: the pristine material is mainly in the α phase, the β phase being only a small contamination.

b. Neutron Data Analysis. The experimental time-of-flight neutron spectra were transformed into energy transfer data, detector by detector, making use of the standard TOSCA-II routines available on the spectrometer. Spectra were added together in two distinct data blocks (i.e., forward-scattering and backscattering, respectively). This grouping procedure was justified by the narrow angular range spanned by the detectors of each block, since the corresponding full-width-at-half-maximum, $\Delta\theta$, was estimated to be only 8°.[15] In this way, we produced double-differential cross-section measurements along the TOSCA-II kinematic paths $Q = Q_{F,B}(E)$ (for forward-scattering and backscattering spectra, respectively) of the sample-plus-can system, plus, of course, the empty can. Data were then corrected for the $(E_1/E_0)^{1/2}$ kinematic factor, and the empty-can contribution was properly subtracted[16] taking into account the E_0-dependent sample transmission. The usual corrections for self-shielding attenuation were carried out, even though the sample exhibited a quite modest scattering power (i.e., $p = 3.2\%$ at $E_0 = 100$ meV), because of the presence of an element with a large absorption cross section such as natural boron ($\sigma_{abs}[B] = 767$ b at $E_0 = 25.3$ meV[17]). This procedures was performed through the analytical approach suggested by Agrawal[18] and by Sears[19] in the case of a flat slablike geometry. Multiple scattering contribution was also evaluated (still according to ref 18) and found to be fully negligible in the energy transfer interval of interest (i.e., 3 meV $< E <$ 350 meV, containing the main spectral features). Processed neutron spectra are reported in Figure 7 as generalized self-inelastic structure factor, $S_s(Q_{F,B}, E)$.[20]

IV. Discussion

Since we have already assigned the main Raman spectral features in section III, we will devote the present section to a short comparison between the Raman data (mixed and β phases) on one side and neutron scattering spectrum (β phase) and ab initio simulated frequencies (α phase) on the other.

The most recent density functional theory calculation of the α phase vibrational modes has been carried out by Dai and coworkers.[21] In their paper, by relaxing the previously suggested structure $P6_1$, they predict a new, higher symmetry $P6_122$ structure, which was subsequently confirmed by the X-ray diffraction determination carried out by Filinchuk et al.[6] on a $Mg(BH_4)_2$ single crystal.

The lattice, bending, and stretching vibrational frequencies are substantially validated by the very complex experimental spectrum that we have detected at low temperature. It is interesting to observe that the results of the theoretical calculations predict more than 10 different components between 2280 and 2380 cm^{-1} for the stretching region of the α phase (cf. Table 2). In addition, the calculated spectrum for lattice modes turned out extremely rich too, with more than 40 different modes, one-half of which could be presumably Raman active. We point out that a more precise comparison could only be performed by knowing the symmetry character of the simulated vibrational modes, which is presently not available.

As for the incoherent neutron spectra displayed in Figure 8, it is important to recall the three main differences[20] with respect to the corresponding low temperature Raman measurements on

β-$Mg(BH_4)_2$: (a) the full first Brillouin zone of the crystal is probed, not only the phonons at the Γ-point, like in Raman scattering. This implies that especially the lattice modes are observed as averaged over their full dispersion curves. (b) Due to the large proton cross section,[17] incoherent neutron scattering is mainly sensitive to the vibrational normal modes involving large H displacements. (c) No selection rule applies. Keeping in mind these simple rules, it is possible to interpret the aforementioned neutron spectra in a straightforward way. In the spectral onset, 3−38 meV (24−306 cm^{-1}), a strong and structured band is measured, showing large intensity differences between backscattering and forward-scattering data. These features are surely ascribable to the lattice phonons, and, due to their dispersions and to the spectrometer energy resolution, no specific assignment is actually possible. Moving to higher energy transfer values, one notes another intense band placed between 44 and 82 meV (355−661 cm^{-1}), peaked at about 65 meV (524 cm^{-1}), and completely missing in the corresponding Raman spectra. For this reason we are convinced that it corresponds to the rigid librations of the $[BH_4]^-$ tetrahedron.[10] Further on, a number of sharp peaks is visible in the 80−183 meV (645−1476 cm^{-1}) range, four of which are particularly strong, namely, those placed at 114 meV (919 cm^{-1}), 139 meV (1121 cm^{-1}), 147−159 meV (1186−1282 cm^{-1}), and 172 meV (1387 cm^{-1}). In this case the assignment is simple, due to the strict correspondence with the Raman peaks related to the $[BH_4]^-$ bending modes and reported in Table 3 (i.e., 1117, 1204, and 1390 cm^{-1}). Finally, no band is observed between 190 and 272 meV (1532−2193 cm^{-1}), while the weak hump between 274 and 330 meV (2210−2262 cm^{-1}) can be easily assigned to the $[BH_4]^-$ stretching modes (see again Table 3).

V. Conclusions

We have measured the low temperature Raman spectra of magnesium borohydride in the mixed (α plus β) phase and the Raman and neutron spectra of the pure β phase. XRD investigation and Raman spectroscopy results revealed that the pristine material is almost in the pure α phase, the β phase being a small contamination. We have shown that the low temperature measurements exhibit a significant band narrowing, revealing a complex structure in both the internal (particularly BH stretching) and the external vibrational modes. The recent ab initio calculations on the α phase by Dai and co-workers provide a set of vibrational frequencies that qualitatively agree with our findings in the mixed phase. The low temperature spectra evidence the splitting of the BH vibrational mode, mainly in the α phase. Such an effect can be related to the degeneracy lifting of the BH vibrational modes caused by the site splitting effect. On the contrary, the correlation field effect should not give a measurable splitting, analogously to the case of simpler borohydrides.[12] Moreover, we observe that the low temperature Raman spectrum shows the presence of 16 different excitation modes, mainly related to the α phase, in the lattice phonon region.

Raman spectroscopy has also been used to follow the α to β phase transition and to investigate the β phase at low temperature. In the latter, both the external and the internal vibrational modes of the $[BH_4]^-$ anion are considerably modified with respect to the mixed phase. The number of external modes turns out to be substantially reduced, while the BH vibrational band results less structured and smoother than that observed in the mixed-phase spectrum.

The neutron spectroscopy experiment basically agrees with the Raman results. In addition, it reveals the presence of an extra band that is interpreted as due to the $[BH_4]^-$ librations.

A more extensive and comprehensive study on $Mg(BH_4)_2$ will surely need further spectroscopic work as well as ab initio calculations of the β phase, including simulated Raman and neutron spectra.

Acknowledgment. This work has been performed within the framework of the EU-FP7 Project NANOHy. The neutron activity has been partially financed by *Consiglio Nazionale delle Ricerche* (CNR, Italy) through the Cooperation Agreement No. 01/9001 between CNR and STFC (U.K.).

Supporting Information Available: Experimental spectrum showing the infrared absorption of the "as prepared" sample. This material is available free of charge via the Internet at http://pubs.acs.org.

References and Notes

(1) Chlopek, K.; Frommen, Ch.; Léon, A.; Zabara, O.; Fichtner, M. *J. Mater. Chem.* **2007**, *17*, 3496.
(2) Soloveichik, G. L.; Gao, Y.; Rijssenbeek, J.; Andrus, M.; Kniajanski, S.; Bowman, R. C.; Hwang, S. J.; Zhao, J. C. *Int. J. Hydrogen Energy* **2009**, *34*, 916.
(3) Konoplev, V. N.; Bakulina, V. M. *Bull. Acad. Sci. USSR Div. Chem. Sci. (Engl. Transl.)* **1971**, *20*, 136.
(4) Li, H. W.; Miwa, K.; Ohba, N.; Fujita, T.; Sato, T.; Yan, Y.; Towata, S.; Chen, M. W.; Orimo, S. *Nanotechnology* **2009**, *20*, 204013.
(5) Her, J. H.; Stephens, P. W.; Gao, Y.; Soloveichik, G. L.; Rijssenbeek, R.; Andrus, M.; Zhao, J. C. *Acta Crystallogr., Sect. B* **2007**, *63*, 561.
(6) Filinchuk, Y.; Černi, R.; Hagemann, H. *Chem. Mater.* **2009**, *21*, 925.
(7) Černi, R.; Filinchuk, Y.; Hagemann, H.; Yvon, K. *Angew. Chem.* **2007**, *46*, 5765.
(8) George, L.; Drozd, V.; Saxena, S. K.; Bardají, E. G.; Fichtner, M. *J. Phys. Chem. C* **2009**, *113*, 486.
(9) Giannasi, A.; Celli, M.; Grazzi, F.; Ulivi, L.; Zoppi, M. *Rev. Sci. Instrum.* **2008**, *79*, 013105.
(10) Allis, D. G.; Hudson, B. S. *Chem. Phys. Lett.* **2004**, *385*, 166.
(11) Racu, A. M.; Schoenes, J.; Lodziana, Z.; Borgschulte, A.; Züttel, A. *J. Chem. Phys. A* **2008**, *112*, 9716.
(12) Harvey, K. B.; McQuaker, N. R. *Can. J. Chem.* **1971**, *49*, 3272. Harvey, K. B.; McQuaker, N. R. *Can. J. Chem.* **1971**, *49*, 3282. Harvey, K. B.; McQuaker, N. R. *J. Chem. Phys.* **1971**, *55*, 4390.
(13) Carbonniere, P.; Hagemann, H. *J. Phys. Chem A* **2006**, *110*, 9927.
(14) Renaudin, G.; Gomes, S.; Hagemann, H.; Keller, L.; Yvon, K. *J. Alloys Compd.* **2004**, *375*, 98.
(15) Colognesi, D.; Celli, M.; Cilloco, F.; Newport, R. J.; Parker, S. F.; Rossi-Albertini, V.; Sacchetti, F.; Tomkinson, J.; Zoppi, M. *Appl. Phys. A.* **2002**, *74*, S64–66.
(16) Paalman, H. H.; Pings, C. J. *J. Appl. Phys.* **1962**, *33*, 2635.
(17) Sears, V. F. *Neutron News* **1992**, *3*, 26.
(18) Agrawal, A. K. *Phys. Rev. A* **1971**, *4*, 1560.
(19) Sears, V. F. *Adv. Phys.* **1975**, *24*, 1.
(20) Mitchel, P. C. H.; Parker, S. F.; Ramirez-Cuesta, A. J.; Tomkinson, J. *Vibrational Spectroscopy*; World Scientific: Singapore, 2005.
(21) Dai, B.; Sholl, D. S.; Johnson, J. K. *J. Phys. Chem C* **2008**, *112*, 4391.
(22) Johnson, J. K. Private communication, 2009.

JP911175N